Journal of Cellular Biochemistry 86:651–664 (2002)

Th1 and Th2 Cytokines Exert Regulatory Effects Upon Islet Microvascular Areas in the NOD Mouse

Gianpaolo Papaccio,[1]* Francesco Aurelio Pisanti,[2] Rosita Di Montefiano,[1] Antonio Graziano,[1] and Michael VG Latronico[3]

[1]Department of Experimental Medicine, Laboratory of Histology and Embryology, School of Medicine, Second University of Naples, 5 via Luciano Armanni, 80138 Naples, Italy
[2]Department of Cell Biology, School of Biological Science, University of Calabria, Cosenza, Italy
[3]I.N.M. Neuromed, 86077 Pozzilli, Isernia, Italy

Abstract In this study, we show that intra- and peri-islet microvascular areas undergo different changes during the islet inflammation in the nonobese diabetes-prone female mice. Actually, although the islet vascular area (IVA) considerably decreases while the infiltration progresses, at 15 weeks of age, the peri-islet vascular bed is unexpectedly and significantly increased. On the contrary, the intra-IVA is significantly decreased, due to vessel dilation. Later, by 20–25 weeks of age, a decrease of both IVA occur, due to a significant islet β cell loss. Moreover, a dramatic fall of natural free radical scavenger values, which, in turn, exert an influence upon vessels, is observed. These effects are completely counteracted by the administration of IL-4, a Th2 protective cytokine; IL-10, another putative Th2 cytokine, exerts direct effects upon endothelial cell (EC) function, as shown by the increase of endothelial nitric oxide synthase (eNOS) mRNA transcripts and by the release of endothelial NO which, in turn, exert vasodilatory effects; moreover, this cytokine significantly upregulates adhesion molecules on endothelia. On the other hand, IL-1β, a Th1 proinflammatory cytokine, dramatically increases nitrite and nitrate levels, as well as inducible nitric oxide synthase (iNOS) transcripts and also upregulates islet ICAM-1 expression as well as circulating ICAM-1 levels. Taken together, our findings clearly show that cytokines and islet endothelia are directly involved in the pathophysiology of the disease. Their reciprocal influence gives new insight to understand the role of microvasculature during islet β cell attack. J. Cell. Biochem. 86: 651–664, 2002.

Key words: islet vessels; free radicals; IL-1β; IL-4; IL-10; eNOS; iNOS; adhesion molecules; NOD mouse

Studies on islet vascular areas (IVA) in multiple low-dose streptozocin-treated (MLDS) mice have demonstrated that their decrease is concurrent with a fall of superoxide dismutase (SOD) levels [Papaccio et al., 1990; Papaccio and Chieffi Baccari, 1992]. Moreover, administration of citiolone, a free radical scavenger, is capable of counteracting and delaying the reduction of IVA in this animal model of type 1 diabetes [Papaccio et al., 1994].

During diabetes development, the involvement of peri-islet vascular bed with respect to the intra-islet vessels and their specific roles remain, however, a neglected topic.

Functional studies have also shown that both acute and chronic hyperglycemia raise islet vascular pressure [Carlsson et al., 1997].

Endothelial cells (ECs) are both a target and a source of several cytokines. In particular, ECs participate in leukocyte recruitment caused by

Abbreviations: CAT, catalase; DC, dendritic cell; EC, endothelial cell; eNOS, endothelial nitric oxide synthase; GPX, glutathione peroxidase; iNOS, inducible nitric oxide synthase; IVA, islet vascular area; MLDS, multiple low-dose streptozocin; NOD, nonobese diabetic mice; NOR, nonobese diabetic resistant mice; SOD, superoxide dismutase; Th1, helper T cells secreting type 1 inflammatory cytokines; Th2, helper T cells secreting type 2 inflammatory cytokines; TNF-α, tumor necrosis factor alpha.

Grant sponsor: Campanian Region; Grant number: L.R. 31.12.1994, n. 41; Grant sponsor: PRIN 1999 (research projects of relevant interest, the Italian Ministry for Research and University).

*Correspondence to: Prof. Gianpaolo Papaccio, Institute of Histology and Embryology, School of Medicine, Second University of Naples, 5 via L. Armanni, 80138 Naples, Italy. E-mail: gianpaolo.papaccio@unina2.it

Received 27 March 2002; Accepted 21 May 2002

DOI 10.1002/jcb.10250

inflammatory cytokines, by producing chemoattractants that activate and attract leukocytes, by expressing adhesion molecules in a regulated way, and by altering blood flow [Mantovani et al., 1992]. IL-1β and TNF-α orient EC function in a proinflammatory sense [Mantovani et al., 1992], while IL-4 and -10 are reported to be Th2 protective cytokines [Rabinovitch, 1988]. In fact, IL-4 has been demonstrated to exert an antidiabetogenic action in nonobese diabetic (NOD) mice [Rapoport et al., 1993] and IL-10 to inhibit Th1 cytokine synthesis [Fiorentino et al., 1989]. In addition to its anti-inflammatory and immunosuppressive property [Moore et al., 1993], IL-10 has been found to be a potent recruitment signal for leukocyte migration in vivo because it is able to highly activate pancreatic ECs and stimulate leukocyte extravasation throughout the pancreas [Wogensen et al., 1993]. Systemic administration of IL-4 [Rapoport et al., 1993], IL-10 [Pennline et al., 1994], or both [Rabinovitch et al., 1995] has been reported to prevent type 1 diabetes or delay autoimmune diabetes recurrence in NOD mice transplanted with syngeneic islets. Studies on transgenic mice have also suggested that IL-10 may promote the early development of autoimmunity [Wogensen et al., 1994], but suppress an already established diabetogenic process [Pennline et al., 1994].

The NOD mouse is a useful animal model of type 1 diabetes, which spontaneously develops a disease very similar to that observed in humans. As yet, the islet and, in particular, the peri-islet microvasculature in this strain have not been fully investigated in relationship with diabetes development. Furthermore, in view of recent studies demonstrating a direct involvement of ECs in the inflammatory process leading to type 1 diabetes [Steiner et al., 1997], islet and peri-islet microvessels may exert a pivotal role in the disease development. Interestingly, it has recently been shown that NOD mouse diabetes-prone females exhibit alterations in islet vessels islets due to an increase in endothelial nitric oxide (eNOS) at this level [Carlsson et al., 1998]. On the other hand, although the microcirculation of the islets of Langerhans has been previously [Bonner Weir and Orci, 1982] examined, it still remains a controversial concept, mainly due to different models of circulation.

Therefore, the aim of this study was to observe the alterations of IVA, in a dynamic time-course study and in relationship with diabetes occurrence, also on the light of cytokine effects.

Our results demonstrate that (i) peri-islet vessels are differently affected by islet inflammation with respect to the intra-islet vascular bed; (ii) Th1 and Th2 cytokines exert strong regulatory effects upon islet vessels as well as adhesion molecules.

RESEARCH DESIGN AND METHODS

Animals

NOD mice were purchased from Bommice (Bomholtgarten, Denmark) and housed in our facility. Animals had free access to tap water and standard laboratory diet and were maintained in pathogen-free conditions. They were subjected to a 12-h light/12-h dark schedule. During the experiments, they were free of viruses or other bacterial pathologies. In this colony, clinically evident diabetes is observable by week 22 in 100% of females but in less than 20% of males, as certified by the farm and observed by us. Nonobese diabetic resistant (NOR), a genetically related strain which is diabetes-resistant (Bommice) of the same age, were used as non-diabetic controls. C57BL6/J mice were used as a further control (Charles River Milan, Italy).

Protocol

NOD females aged 5, 15, 20, and 25 weeks ($n = 6$ animals per each age) were used for the experiment. Animals were decapitated under anesthesia, and pancreas was removed and processed for histological and enzymatic assays.

IL-1β, -4, and -10 Treatment In Vivo

Four-week-old NOD, NOR, and C57BL6/J mice received intraperitoneal injections of 500 U (50 ng) murine rIL-4, rIL-10, or rIL-1β (Boehringer-Mannheim, Biochemicals, Milan, Italy) twice weekly. Control animals received only the vehicle. Five animals of each group were sacrificed at week 5. At the end of the 11-week treatment period (week 15) and at week 20 and 25, the remaining mice ($n = 5$ per each time point per strain) were killed and each pancreas processed as described below.

Evaluation of Glycemia

Blood glucose levels were checked before the start of the experiments in all the animals and every week using the hexokinase method (Boehringer-Mannheim, Germany). Animals

were considered hyperglycemic when their nonfasting blood glucose levels were higher than 8 mmol/L but lower than 12 mmol/L in two successive determinations. Mice were considered diabetics when their blood glucose levels exceeded 12 mmol/L.

Evaluation of Vascular Area in Pancreatic Islets

For light microscopic observations in order to distinguish ECs, one part of the pancreas was used for immunocytochemistry in order to detect the expression of von Willebrand factor (vWF), using fluorescein isothiocyanate (FITC)-conjugated antibody (Sigma, Milan), anti MIDC-8, and anti-CD13 (clone ER-BMDM1, rat IgG2a) (BMA Biochemicals, Augst, Switzerland), which selectively strain dendritic cells (DC), all processed using standard procedures. The other part of each pancreas was stained for alkaline phosphatase using the method described by Gomori [1941]. Each section was treated for 40 min with a solution of 16.3 mmol/L sodium β-glycerophosphate, 16.1 mmol/L sodium diethylbarbiturate, 45.3 mmol/L calcium chloride, and 3.3 mmol/L magnesium sulphide dissolved in distilled water and adjusted to pH 9.4 at room temperature. The slides were then rinsed in distilled water and transferred to a solution containing 68.7 mmol/L cobalt nitrate in distilled water for 5 min. The sections were then rinsed again in distilled water for 1 min and placed for 2 min in a solution containing 104 mmol/L yellow ammonium sulphide.

In order to measure islet parenchymal area and total area of islet vascular bed, serial sections were performed. At least 20 islets from each pancreas were viewed under a light microscope (at a magnification of 400 ×) linked to a videoanalyzer (Image-Brock Analysis, St. Catherine, Ontario, Canada). Measurements were made using a dedicated, specific software by selecting in the serial sections the vascular beds, in order to obtain the total vascular area of each section. The measurements were then collected and compared to previously obtained standards (made from controls) for settings. Each measure was repeated by two different technicians and compared. Only the average measure numbers for each animal and the average measure numbers obtained for each group were given. Also the number of endocrine cells present in each islet was detected. For this purpose, the nuclei of endocrine cells (infiltrating mononuclear cells, when found, were easily identified and not taken into account) within each section were counted. All endocrine cells were counted, on the basis of specific antibodies directed against insulin, glucagons, and somatostatin (Dako, Milan, Italy), processed using standard procedures. Furthermore, the peri-islet vascular bed was also measured separately from the intra-islet vascular bed in order to study possible differences.

Assay of Islet SOD, CAT, and GPX Levels

Islets were isolated from pancreas using standard techniques. Briefly, islets were isolated by ductal injection of collagenase type V solution (Sigma, Milan, Italy; 1.6 mg/ml in HBSS). Islets from 25-week-old animals were pooled in order to obtain a sufficient number of islets. After incubation for 45 min (37°C), the islets were enriched by centrifugation on a Ficoll density gradient (Ficoll 400, Sigma) and then harvested by handpicking under a stereomicroscope. The extraction medium for the measurements of SOD, catalase (CAT), and glutathione peroxidase (GPX) activities was 0.1 M sodium-phosphate buffer at pH 7.0. SOD assay [Papaccio et al., 1994] was based on the ability of the enzyme to inhibit the auto-oxidation of pyrogallol as previously described by Marklund and Marklund [1974]. Results are given as units per milligram (U/mg) of protein (means of triplicates with an intra-assay variation coefficient of 2.7%). The detection limit was found to be 2 U/mg protein [Oellerich et al., 1980]. The concentration of proteins was determined by Lowry's method [Lowry et al., 1951].

For CAT and GPX assays, the procedures were those described by Cornelius et al. [1993]. Spectrophotometric measurements were carried out at 25°C. CAT and GPX activities are expressed as U/mg protein.

Islet EC Culture

To examine the inducible nitric oxide synthase (iNOS) and the eNOS levels at the islet level, endothelia of pancreatic islets were isolated as above described from each animal group. Islets were collected, washed, and then handpicked, resuspended in the medium (RPMI 1640) containing 10% fetal calf serum (Gibco, Milan, Italia), 60U/ml penicillin, and 100 μg/ml streptomycin and then cultured in a 2% gelatin-coated T25 flask (Falcon, Milan, Italy) at 37°C. After 5-day culture, islet ECs and fibroblasts grew out from adherent islets. Dynabeads were

coated with Acetylated LDL (A-LDL) (Sigma, Milan), the flasks washed twice and incubated with A-LDL-coated dynabeads for 60 min, kept at 4°C during separation, then at room temperature with gentle shaking. After washing, the cells were detached by trypsin/EDTA and transferred into a 10-ml plastic tube. The EC bound with dynabeads were collected using magnetic particle concentrator (Dynal A.S., Norway), while cells without bound dynabeads (probably fibroblasts) were collected and used as negative control. The A-LDL helps to confirm the identity of ECs. The purified islet ECs were cultured in the same medium, as above, containing also 40 U/ml heparin (Roche, Switzerland) and 100 μg/ml endothelial growth supplement (ECGS) (Sigma), and then seeded in a gelatin-coated T25 flask. Cells were cultured at 37°C in a 5% CO_2 incubator and the medium changed every 3 days. Cytokines, including IL-1β, -10, and -4 were added to the medium, in different cultures (at the dose of 50 U/ml each), and the culture was continued for 6 days, with the medium changed on day 2 and 4. In order to avoid fibroblast growth, iodoacetic acid (4 μg/ml) was added to cultures.

EC Proliferation

EC proliferation was measured by the 3-(4,5-dimethylthiazolyl)-2-5-dipheny-2H-tetrazolium-bromide (MTT) assay. ECs were seeded in a gelatin-coated 96-well plate at a cell density of 10^3 cells/well. Cells were grown in RPMI 1640 containing 20% FCS plus 100 μg/ml ECGS (Sigma, Milan, Italy). After 1, 3, 5, and 7 days of culture, cells were incubated with the MTT solution (0.5% 50 μl/well) for 4 h. During this incubation period, a water-insoluble formazan dye is formed. After solubilization, the formazan dye is quantitated using a scanning multiwell spectrophotometer (ELISA reader) at 570 nm. The absorbance revealed directly correlates to the cell number. The results were expressed as optical density (OD) at 570 nm.

Isolation of RNA and Reverse Transcriptase-Polymerase Chain Reaction (RT-PCR) Analysis

RNA was extracted from islet EC cultures using the guanidinium thiocyanate method [Chirgwin et al., 1979], modified as follows: ECs were homogeneized in 4 mol/L guanidinium thiocyanate solution containing 17 mmol/L sodium *N*-lauroylsarcosine, 25 mmol/L sodium citrate, 0.1 mol/l 2-ME, and 0.1% Antifoam A, 30% aqueous emulsion (Sigma, Milan, Italy), then precipitated with ethanol, pelleted, and re-extracted with 8 mol/L guanidine hydrochloride: 0.5 mol/L EDTA (19:1). After pelleting and drying, samples were extracted twice with phenol:chloroform (1:1) and precipitated with ethanol. cDNA synthesis was carried out on total RNA from each animal with superscript reverse transcriptase kit (Invitrogen, Milan, Italy) by using oligo $(dt)_{12-18}$ and Moloney murine leukemia virus reverse transcriptase (20 U) in a 25 μl reaction at 37°C for 1.5 h. The reverse transcriptase (RT) reaction containing cDNA was diluted 1:30, 1:90, and 1:270 in sterile H_2O. Polymerase chain reaction (PCR) amplification was carried out on the cDNA using 3 μl of each dilution of cDNA in a 20 μl reaction with 80 ng of each primer, 0.25 mmol/l of each dNTP, 2.5 μCi of [-^{32}P] dCTP (3,000 Ci/mmol; DuPont-NEN, Milan, Italy), 1 U of AmpliTaq (Perkin-Elmer/Cetus, Monza, Italy), and 3 mmol/l $MgCl_2$. The sequences of the specific oligonucleotide primer pairs, 5′ and 3′, were as follows: for iNOS, sense 5′-AGC TTC TGG CAC TGA GTA AAG ATA A-3′ and antisense 5′-TTC TCT GCT CTC AGC TCC AAG-3′; for eNOS, sense 5′-ACC AGC CAG CTG GTG CGC TAC-3′; antisense 5′-CTC CAG GTG CTT CAT GAA AGA-3′, together with primers for cyclophilin, GAC AGC AGA AAA CTT TCG TGC-5′ and TCC AGC CAC TCA GTC TTG G-3′. Samples were amplified through 40 cycles at 94°C for 20 s, 60°C for 20 s, and 72°C for 30 s in a Gene Amp PCR System 9600 (Perkin-Elmer/Cetus, Monza, Italy). The semiquantitative PCR reaction was electrophoresed on 1.5% agarose gels and transferred to nylon membranes, and ^{32}P incorporation in cytokine and cyclophilin DNA bands was determined by phosphoimager analysis. The values obtained of PCR product were normalized as a percentage of 32P incorporated in cyclophilin PCR product amplified from the same cDNA preparation. In these experiments, the template used for the PCR amplification was cDNA from NOD splenocytes activated with concavalin A for 3 days to express the different cytokine messages. Also, this cDNA was used as a positive control in all PCR runs. Under the conditions used, the PCR product signal was proportional to the amount of RNA/cDNA subjected to PCR amplification. All PCR products compared were produced in the same PCR run. The intensities of the bands were quantified in an Ultrascan XL Enhanced Laser densitometer

(LKB, Bromma, Sweden) and expressed in arbitrary units of OD.

Plasma $NO_2 + NO_3$ Assay

Nitrite (NO_2) and nitrate (NO_3), stable metabolites of nitric oxide (NO), were measured in plasma samples belonging to the islet vessels. Blood was collected directly from islets using the technique described by Carlsson et al. [1997], using the Griess reagent (commercial Kit, Sigma, Milan, Italy), and their concentrations were calculated from a standard curve for spectrophotometric absorbance at 540 nm generated for increasing amounts of nitrites. The intra- and interassay coefficient of variation was 3 and 6%, respectively. Recoveries of nitrites and nitrates in our samples were 90 and 95%, respectively. Values were given as micromole per liter (μmol/L).

Circulating ICAM-1 Levels

Soluble ICAM-1 activity was assayed using the ELISA CD54 kit (Endogen, Woburn, MA). Blood samples from each animal were collected from the retro-orbital plexus and processed following the kit's instructions. Values were expressed as nanogram per milliliter (ng/mL).

ICAM-1 Expression

Samples from the tail of each pancreas were collected and kept frozen in liquid nitrogen. Randomly selected cryocut sections were stained by the avidin-biotin peroxidase indirect staining method.

The monoclonal antibody anti-ICAM-1 was a rabbit anti-rat (Santa Cruz Biotechnology, CA). The secondary antibody was biotinylated goat anti-mouse antibody. As a negative control, the primary Ab was replaced with goat non-immune serum. Sections of 5-μm thickness were examined for semiquantitative analysis. The immunoreactive cells on alternate sections were determined at a magnification of 400 × using an eyepiece with a square-ruled grid with a total area of 0.062 mm^2 and were counted with the M4 image analysis system (Imaging-Brock University, St. Catherin, Ontario, Canada) in 60 different areas. This allowed the calculation of immunoreactive cells/$mm^2 \pm$ SEM. The observations were carried out blindly by three different researchers.

Statistical Analysis

Values are given as means ± SD. Student's t test with Bonferroni correction was used for statistical analysis: the level of significance was set at $P < 0.05$. When multiple comparisons between data were performed, analysis of variance (ANOVA) was used.

RESULTS

Glycemia

Results are shown in Table I. Untreated NOD animals are normoglycemic at week 5, after which blood glucose levels start to increase ($P < 0.01$ week 15 vs. 5-week-old NOD animals). Twenty- and 25-week-old NOD mice are overtly diabetic, since their blood glucose values considerably exceed 12 mmol/L ($P < 0.0001$ vs. all animal groups). IL-4 as well as IL-10 treated animals show normal blood glucose values throughout the experiment (see Table I), demonstrating the protection exerted by these cytokines against type 1 diabetes. Oppositely, IL-1β administration does not modify the course of blood glucose values of NOD animals, which were comparable to those found in untreated controls. Insulin treatment was needed when blood glucose values exceeded 18–20 mmol/L of glucose in two successive measurements.

Both NOR and C57BL6/J mice were constantly normoglycemic throughout the experiment.

TABLE I. Blood Glucose Values

Strain	Week 5	Week 15	Week 20	Week 25
NOD (untreated)	5.3 ± 0.5	8.4 ± 2.2*	19.2 ± 3.8**	22.9 ± 3.1**
NOD (+ IL-4)	5.4 ± 0.6	5.6 ± 0.8	5.4 ± 1.0	5.8 ± 1.0
NOD (+ IL-10)	5.2 ± 1.0	5.4 ± 1.2	5.3 ± 1.9	5.6 ± 1.2
NOD (+ IL-1β)	5.2 ± 1.2	8.0 ± 2.4*	18.2 ± 5.5**	20.6 ± 3.4**
NOR	4.8 ± 0.6	4.5 ± 0.5	5.0 ± 0.8	5.1 ± 1.0
C57	4.9 ± 0.6	5.3 ± 1.0	5.2 ± 0.8	5.3 ± 1.0

*$P < 0.01$ vs. week 5.
**$P < 0.0001$ vs. all week groups.
Values expressed as mmol/L, are means ± SD.

IVA

Gomori's method for alkaline phosphatase stains ECs belonging to islet, peri-islet, and pancreatic vessels. Endothelia are easily differentiated from A cells, which also are stained with this method, by their elongated shape and darker color [Svensson et al., 1988; Papaccio et al., 1994].

The percentage of islet area occupied by vessels is shown in Figure 1a. At week 5, untreated NOD as well as NOR and C57Bl6/J mice show that total IVA represents roughly 4% of the islet parenchymal area. At this time, both intra-islet and peri-islet vascular bed of NOD mice show a normal appearance (Fig. 2), comparable to that seen in NOR and C57Bl6/J animals. A significant alteration of the islet vascular bed is observable by week 15 in untreated NOD animals (Fig. 3). Actually, at this time, total IVA is reduced to 3.6% of the islet parenchymal area, though a peri-islet vascular dilation is observed concomitant to a decrease of the intra-islet vascular bed (Fig. 1b). By week 20, IVA decreases dramatically to 1.6%. In particular, both intra-islet and peri-islet vascular bed (Fig. 1c) become significantly lower ($P < 0.001$) than that measured at week 15; interestingly, this happens concomitantly to the expected significant decrease in endocrine cell numbers ($P < 0.001$) (Table II). At 25 weeks, islets are retracted due to islet β cell death and disappearance.

Interestingly, IL-4 treated animals do not show the above-described alterations: peri- and intra-IVA remain unchanged after treatment and the vascular area is comparable with that found in young nondiabetic animals and in NOR

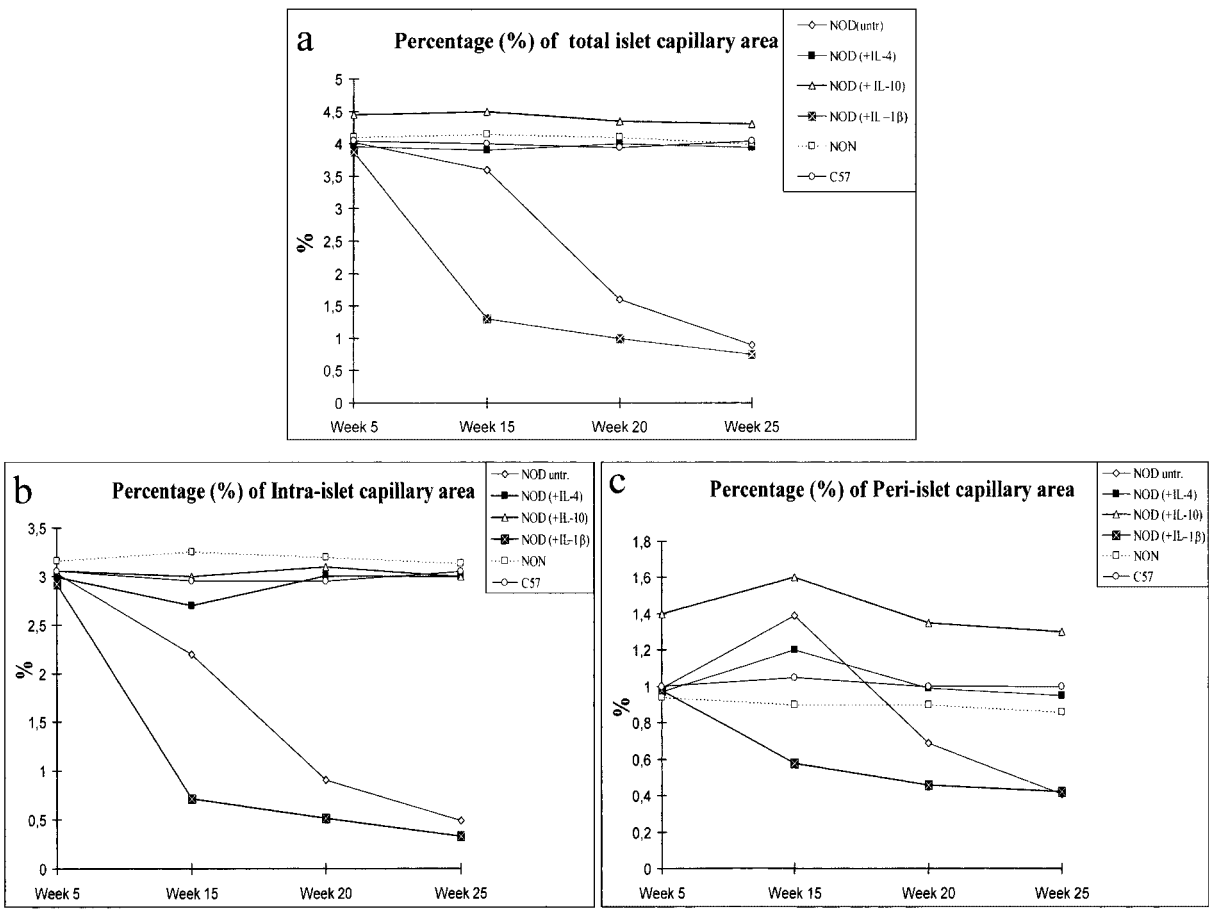

Fig. 1. (**a**) Figure showing the percentage (%) of total islet area occupied by vessels. Data are given as means ± SD; (**b**) figure showing the percentage (%) of intra-islet vascular bed. Data are given as means ± SD; (**c**) figure showing the percentage (%) of peri-islet vascular bed. Data are given as means ± SD.

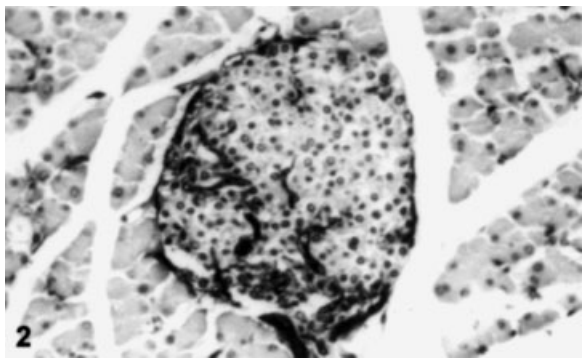

Fig. 2. Light micrograph showing a 5-week-old NOD mouse pancreatic section stained with Gomori's method for alkaline phosphatases. The islet is of normal appearance with unaltered islet and peri-islet vascular bed (original magnification 380 ×).

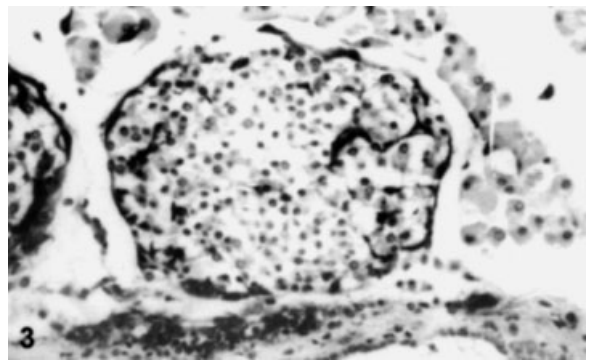

Fig. 3. Light micrograph showing a 15-week-old NOD mouse pancreatic section stained with Gomori's method for alkaline phosphatases. The islet shows an increased peri-IVA with dilation of vessels and an initial reduction of the intra-IVA. (original magnification 380 ×).

and C57BL6/J control animals, demonstrating that in vivo treatment with this cytokine is also able to counteract islet vascular changes.

IL-10 administration to NOD animals exerts both protective effects upon the islets, which are devoid of infiltration, and direct effects upon endothelia and vessels which are dilated (Fig. 4), in particular the percentage of total IVA is increased in these animals (4.45%), with respect to controls and IL-4 treated animals. The peri-IVA represents the vascular district, which shows the major effects of IL-10 administration; dilation of these vessels is slightly higher, in absolute values, with respect to that observed in untreated NOD controls.

Oppositely, IL-1β accelerates vascular alterations: at week 15, IVA values fall to 1.3%; at week 20, the value is 0.98%; and at week 25, it is

TABLE II. Table Showing the Percentage of Intra-Islet (I), Peri-Islet (P), and Total (T) Vascular Area

Strain	Week 5	Week 15	Week 20	Week 25
NOD untreated	E, 201 ± 15 (T = 4.02%) I, 3.03% P, 0.99%	170 ± 15 (T = 3.60%) 2.21%** 1.39%***	102 ± 9 (T = 1.60%) 0.91%***** 0.69%	42 ± 6 (T = 0.90%) 0.49%******* 0.41%********
NOD (+ IL-4)	E, 195 ± 12 (T = 3.96%) I, 2.99% P, 0.97%	190 ± 8 (T = 3.90%) 2.70% 1.20%	222 ± 16 (T = 4.00) 3.01% 0.99%	202 ± 14 (T = 3.95%) 3.00% 0.95%
NOD (+ IL-10)	E, 220 ± 12 (T = 4.02%) I, 3.01% P, 1.01%	238 ± 18 (T = 4.1%) 2.8% 1.3%	220 ± 14 (T = 4.04) 3.01% 1.03%	210 ± 8 (T = 4.10%) 3.1% 1.0%
NOD (+ IL-1β)	E, 200 ± 8 (T = 3.88%) I, 2.92% P, 0.98%	100 ± 6 (T = 1.3) 0.72% 0.58%	53 ± 5 (T = 0.98%) 0.52% 0.46%	43 ± 7 (T = 0.75%) 0.33% 0.42%
NOR	E, 190 ± 22 (T = 4.02%) I, 3.16% P, 0.96%	200 ± 26 (T = 4.05%) 3.20% 0.94%	226 ± 22 (T = 4.12%) 3.24% 0.92%	222 ± 18 (T = 4.01%) 3.18% 0.90%
C57	E, 208 ± 10 (T = 4.05%) I, 3.05% P, 1.00%	216 ± 14 (T = 4.00%) 2.95% 1.05%	209 ± 15 (T = 3.95%) 2.95% 1.00%	214 ± 10 (T = 4.05%) 3.05% 1.00%

*$P < 0.01$ vs. weeks 5, NOR and C57.
**$P < 0.01$ vs. weeks 5, NOR and C57.
***$P < 0.05$ vs. weeks 5, NOR and C57.
****$P < 0.001$ vs. week 15.
*****$P < 0.001$ vs. weeks 5 and vs. NOR and C57.
******$P < 0.0001$ vs. all groups.
*******$P < 0.0001$ vs. all groups.
********$P < 0.0001$ vs. all groups.
E = Average number of endocrine cells per islet. (Data are given as means ± SE.)

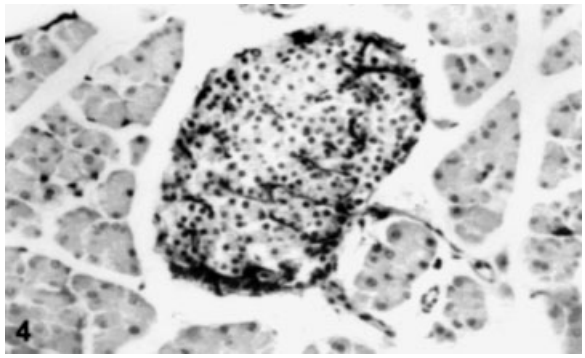

Fig. 4. Light micrograph showing a 20-week-old NOD mouse treated with IL-10. The pancreatic section, stained with Gomori's method for alkaline phosphatases, shows a normal islet without signs of insulitis or parenchymal alteration. Islet and, above all, peri-islet vascular bed are extended and dilated (original magnification 380 ×).

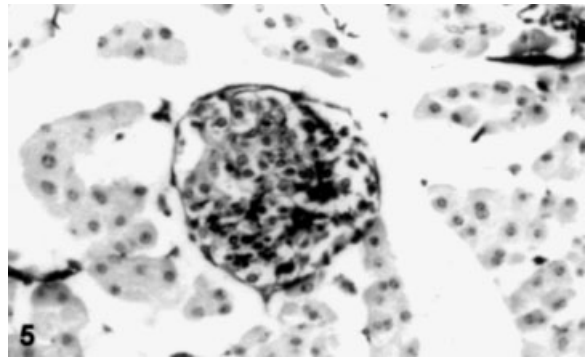

Fig. 5. Light micrograph showing a 20-week-old NOD mouse treated with IL-1β. The pancreatic section, stained with Gomori's method for alkaline phosphatases, shows a retracted and atrophied islet of Langerhans with cytoarchitectural derangement (original magnification 380 ×).

further decreased. As for untreated NOD mice, a significant decrease of both peri- and intra-islet vascular bed is observed at week 20 and 25 also in these animals ($P < 0.001$) concomitant to the decrease of the endocrine cell numbers ($P < 0.001$) (Table II). Moreover, at week 20 (Fig. 5), islets often appear atrophied with cyto-architectural derangement. NOR and C57Bl6/J mice do not show significant alterations of their islet and peri-islet vascular bed during the experiment.

For EC identification, additional analysis using FITC-conjugated antibodies for von Willebrand Factor (Fig. 6) demonstrate the same pattern observed using the Gomori's method. Moreover, both MIDC-8 and CD13 antibodies, specific for DC, being completely negative, demonstrate that these elements were not detected.

SOD, CAT, and GPX Levels in Pancreatic Islets

Results are summarized in Table III. SOD levels are significantly lower in NOD animals when compared to NOR and C57BL6/J animals ($P < 0.0001$ vs. all animal groups). Moreover, within the NOD group, values are significantly decreased by week 15, and by week 25 become

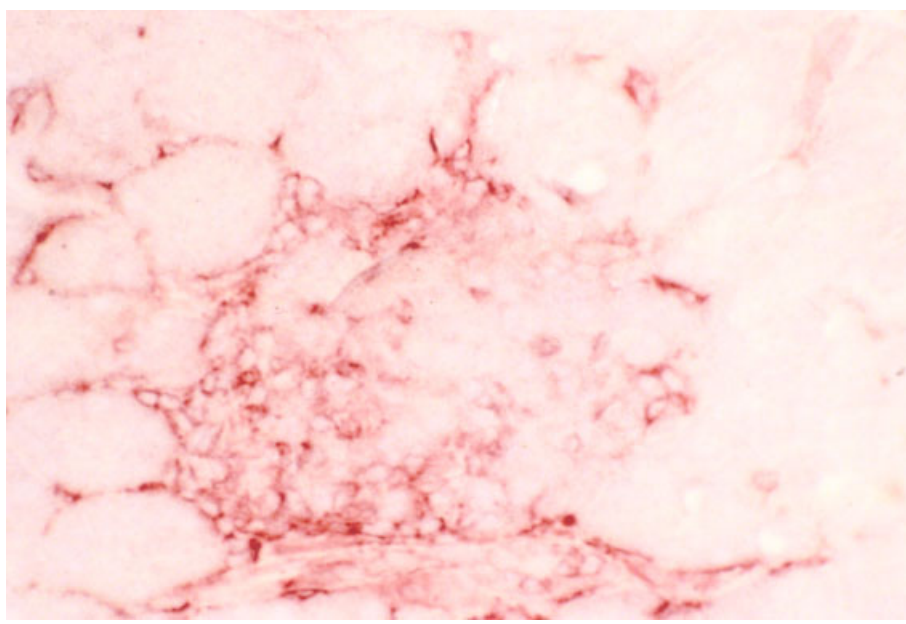

Fig. 6. Light micrograph showing von Willebrand Factor (vWF) islet endothelia positivity in a 5-week-old NOD animal. The figure represents three independent experiments. [Color figure can be viewed in the online issue, which is available at www.interscience.wiley.com.]

TABLE III. SOD, CAT, and GPX levels in NOD, NOR, and C57BL6/J Animals

	SOD	CAT	GPX
NOD (untreated)			
Week			
5	12.1 ± 0.5	15 ± 0.8	22 ± 1.0
15	7.2 ± 0.4*	9 ± 0.5***	15 ± 1.0*****
20	6.0 ± 0.5*	9 ± 0.5***	14 ± 1.0*****
25	2.1 ± 0.1**	7 ± 0.4****	12 ± 0.6******
NOD (+IL-4)			
Week			
5	12.2 ± 0.6	1.6 ± 0.6	22 ± 1.0
15	12.0 ± 0.6	16 ± 0.4	21 ± 1.0
20	11.5 ± 0.5	15 ± 0.8	22 ± 1.0
25	12.1 ± 0.7	15 ± 0.6	21 ± 2.0
NOD (+IL-10)			
Week			
5	12.2 ± 1.4	15 ± 0.8	21 ± 1.0
15	12.5 ± 0.9	15 ± 1.2	21 ± 1.0
20	12.0 ± 0.6	16 ± 0.4	22 ± 2.0
25	11.5 ± 1.5	15 ± 0.8	22 ± 1.5
NOD (+IL-1β)			
Week			
5	25.0 ± 1.0	19 ± 1.0	28 ± 2.0
15	6.0 ± 1.0*	8 ± 1.2****	14 ± 2.0*****
20	1.5 ± 0.3**	6 ± 1.2****	9 ± 2.0******
25	1.3 ± 0.5**	6 ± 1.4****	8 ± 1.0******
NOR			
Week			
5	100 ± 10	17 ± 1.1	22 ± 2.0
15	104 ± 16	16 ± 1.0	22 ± 2.0
20	100 ± 10	14 ± 1.0	22 ± 2.0
25	98 ± 6	16 ± 2.0	26 ± 2.0
C57			
Week			
5	115 ± 11	16 ± 2.0	26 ± 3.0
15	117 ± 15	16 ± 3.0	22 ± 2.0
20	15 ± 10	15 ± 2.0	24 ± 2.0
25	113 ± 10	15 ± 2.0	25 ± 3.0

*$P < 0.01$ vs. NOD (untreated) week 5, NOD (+IL4), NOD (+IL-10).
**$P < 0.001$ vs. all groups.
***$P < 0.01$ vs. NOD (untreated) week 5, NOD (+IL-4), NOD (+IL-10).
****$P < 0.001$ vs. all groups.
*****$P < 0.05$ vs. NOD (untreated) week 5, NOD (+IL-4), NOD (+IL-10).
******$P < 0.001$ vs. all groups.
Values are expressed as U/mg protein ± SD.

dramatically low ($P < 0.01$ vs. week 5). CAT and GPX levels also start to fall from week 15 to 25 in NOD animals ($P < 0.01$ vs. week 5), suggesting that the whole antioxidant capacity is considerably lowered by diabetes development.

IL-4 as well as IL-10 treated animals do not show changes in antioxidant enzyme levels, but IL-1β increases SOD, GPX, and CAT levels early on, at week 5, after which all antioxidant enzyme values are dramatically lowered.

SOD, CAT, and GPX levels remain unchanged throughout the experiment in NOR and C57 animals.

Characterization of IEC

Immunocytochemistry confirmed the high purity of the endothelial cultures in which cells obtained from NOD animals and controls expressed vWF molecules. The FITC fluorescence profiles (not shown) demonstrated that more than 90% of cultured cells expressed positivity to vWF. No age variation was found during the experiments.

EC Proliferation Capacity

Proliferation rate in cultured ECs was quantified by BrdU specific ELISA method. Significant cell proliferation was observed around adherent islets as well as from purified endothelia. MTT assay reveals that islet endothelia proliferation capacity of NOD animals was comparable to that obtained from endothelia of controls.

RT-PCR Analysis for iNOS and eNOS

In this study, a specific PCR product was detected in all samples analyzed, belonging to cultures of ECs for eNOS. On the contrary, only IL-1β significantly enhances iNOS (OD = 5.7 ± 0.8 in 15-week-old NOD IL-1β-treated animals with respect to OD = 1.7 ± 0.5 in 15-week-old NOD control). In Figure 7, mRNA transcripts of eNOS are observable; they are significantly increased in ECs belonging to NOD of 15 (OD = 5.8 ± 1.2) ($P < 0.01$ with respect to 5-week-old NOD animals) and 20 week (OD = 7.5 ± 1.0) ($P < 0.001$ with respect to 5-week-old animals), and in IL-10 treated NOD animals (OD = 5.6 ± 0.6) ($P < 0.01$ with respect to all groups). In particular, ECs of 20-week-old NOD show the highest expression (OD = 8.1 ± 1.4). ECs of 15-week-old NOD show an expression of the same extent of those treated with IL-10, demonstrating that this cytokine exerts a specific stimulation on the messenger. In Figure 8, mRNA transcripts of iNOS are clearly observable only in the line belonging to islets of animals treated with IL-1β.

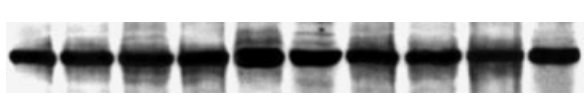

Fig. 7. Expression of eNOS mRNA in islet endothelial cells (ECs). Lane 1: C57BL6/J; lane 2: NOR; lane 3: NOD 5-week old; lane 4: NOD 15-week old; lane 5: NOD 20-week old; lane 6: NOD 25-week old; lane 7: NOD 5-week old + IL-1β; lane 8: NOD 15-week old + IL-1β; lane 9: NOD 20-week old + IL-4; lane 10: NOD 20 week-old + IL-10. The figure represents three independent experiments.

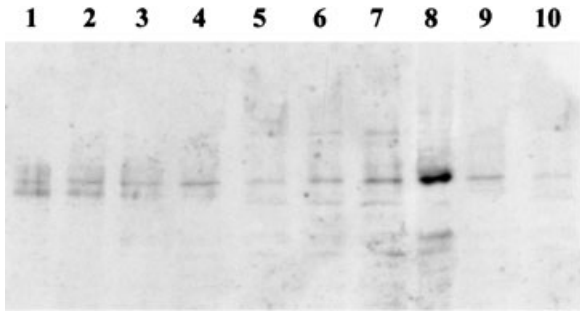

Fig. 8. Expression of iNOS mRNA in islet endothelial cells (ECs). Lane 1: C57BL6/J; lane 2: NOR; lane 3: NOD 5-week old; lane 4: NOD 15-week old; lane 5: NOD 20-week old; lane 6: NOD 25-week old; lane 7: NOD 25-week old; lane 8: NOD 15-week old + IL-1β; lane 9: NOD 15-week old + IL-4; lane 10: NOD 15-week old + IL-10. The figure represents three independent experiments.

Plasma Nitrites and Nitrates

Levels of plasma $NO_2 + NO_3$, a marker for local NO production, indicate that the release of this potent modulator of vascular response is increased in untreated NOD animals by week 15 (Table IV). At week 20, values start to decrease, though it is still higher with respect to that found at week 5 and in controls or in animals treated with IL-4. The highest increase of plasma nitrites and nitrates are seen at week 15, concomitantly to the increase (i.e., vasodilation) of the peri-IVA (see above). Also in IL-10 treated animals, an increase of NO stable metabolites is found, further demonstrating a direct effect of this cytokine upon endothelial function.

IL-1β-treated animals also show increase levels of nitrite and nitrate. C57Bl6/J and NOR animals do not show changes of NO metabolites.

Adhesion Molecule Observations

Interestingly, adhesion molecules were upregulated by IL-1β. In particular, while IL-4 downregulates (Table V) and IL-10 does not exert significant effects upon sICAM-1, IL-1β strongly enhances ($P < 0.001$, Table V) circulating adhesion molecule levels. Moreover, while IL-10 enhances ICAM-1 expression on islet endothelia (Fig. 9) and on scattered cells, IL-1β significantly increases adhesion molecule expression on islet cells (Fig. 10), but not on islet endothelia. Therefore, a different target between the two cytokines is observed: in fact, IL-10 exerts a specific ICAM-1 upregulation upon islet endothelia, while IL-1β exerts its activity upon circulating (Table V) and islet ICAM-1 molecules.

TABLE IV. Plasma $NO_2 + NO_3$ Levels in NOD, NOR, and C57BL6/J Animals

NOD (untreated)	
Week	
5	18.6 ± 2.5
15	28.2 ± 6.4*
20	23.8 ± 5.5**
25	18.6 ± 2.1
NOD (+ IL-4)	
Week	
5	17.2 ± 1.6
15	18.0 ± 2.6
20	17.5 ± 1.5
25	18.1 ± 1.7
NOD (+ IL-10)	
Week	
5	22.6 ± 3.8**
15	28.5 ± 5.9*
20	29.0 ± 3.6*
25	26.5 ± 2.5*
NOD (+ IL-1β)	
Week	
5	18.2 ± 3.0
15	27.5 ± 4.0*
20	23.0 ± 3.3**
25	18.3 ± 3.5
NOR	
Week	
5	18.6 ± 2.1
15	18.0 ± 3.0
20	18.0 ± 2.6
25	18.4 ± 3.0
C57	
Week	
5	17.8 ± 2.2
15	17.6 ± 3.0
20	18.4 ± 3.6
25	18.6 ± 4.0

*$P < 0.001$.
**$P < 0.05$.
Values are expressed as μmol/L and are means ± SD.

DISCUSSION

In this study, we show that intra- and peri-islet vessels are differently affected during the natural history of type 1 diabetes development in the NOD mouse and that significant alterations of the percentage of the IVA occupied by vessels occur, as previously reported for MLDS-treated mice [Papaccio et al., 1994]. We also show that Th1 and Th2 cytokines exert strong regulatory effects on islet vessels.

Actually, insulitis progression and, in particular, recruitment of infiltrating cells from extrapancreatic areas, leading to peri-islet inflammation and, then, to intra-islet infiltration, are responsible for significant, but different vascular alterations.

TABLE V. Levels of Circulating Adhesion Molecules (cICAM-1) in NOD, NOR, and C57BI6/J

NOD (untreated)	
Week	
5	35 ± 4
15	36 ± 8
20	40 ± 12
25	42 ± 9
NOD (+ IL-4)	
Week	
5	39 ± 7
15	27 ± 5
20	18 ± 6*
25	16 ± 2**
NOD (+ IL-10)	
Week	
5	35 ± 6
15	30 ± 8
20	34 ± 6
25	31 ± 4
NOD (+ IL-1β)	
Week	
5	39 ± 7
15	270 ± 22**
20	288 ± 3.3**
25	308 ± 3.5**
NOR	
Week	
5	38 ± 8
15	38 ± 6
20	39 ± 8
25	40 ± 10
C57	
Week	
5	37 ± 8
15	39 ± 8
20	40 ± 6
25	42 ± 9

*$P < 0.01$ vs. week 5, NOD untreated, NOD+ IL-10, NOR, and C57 and $P < 0.001$ vs. NOD+ IL-1β.
**$P < 0.001$ vs. week 5, NOD untreated, NOD+ IL-4, NOD+ IL-10, NOR, and C57.
Values are expressed as ng/mL and are means ± SD.

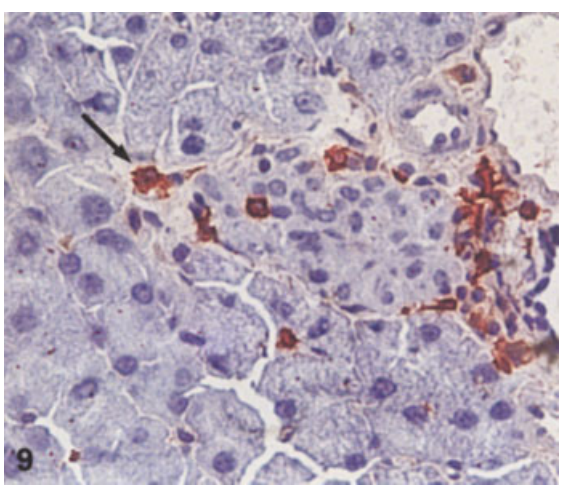

Fig. 9. Light micrograph of an islet belonging to animals treated in vivo with IL-10, showing ICAM-1 expression on endothelia (arrow). (Original magnification 450 ×.) [Color figure can be viewed in the online issue, which is available at www.interscience.wiley.com.]

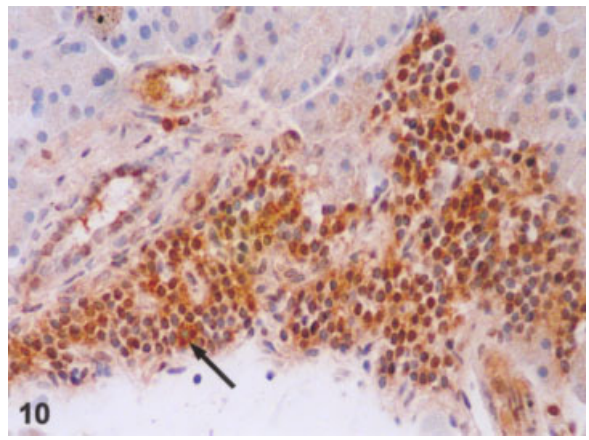

Fig. 10. Light micrograph of an infiltrated islet cell belonging to animals treated in vivo with IL-1β, showing ICAM-1 expression (arrow). (Original magnification 400 ×.) [Color figure can be viewed in the online issue, which is available at www.interscience.wiley.com.]

Interestingly, we have found that in the NOD mouse, total IVA starts to decrease by week 15, mainly due to a significant decrease of intra-islet vascular bed: in fact peri-islet vessels unexpectedly increase their area, which falls only later. By week 25, this decrease is concomitant to a dramatic fall of endocrine cell numbers, due to the disappearance of islet β cells. Earlier studies suggested that marginating monocytes present within the vasculature of the pancreas, but not within other organs, are stimulated to release vasoactive agents, including E-series prostaglandins, which release vascular leakage by inducing transient gaps between ECs [Carlsson et al., 1998; Papaccio et al., 1998].

These vascular alterations happen concomitantly to the recruitment of infiltrating cells: in fact, as infiltrating cells are recruited, a dilation of peri-islet vascular bed takes place, leading to an increase of their vascular area. This recruitment is over by week 20–25, when a dramatic fall of islet endocrine cell numbers and marked islet derangement occur.

Moreover, a significant fall of natural oxygen free radical scavengers, namely CAT, GPX, and SOD, whose levels are considerably low in NOD animals [Papaccio et al., 1995], further supports our findings: free radicals not only facilitate islet β cell death, but have been also found to be potent regulators of the microcirculation and may, therefore, mediate the vascular effects of diabetes development [Gryglewski et al., 1988; Rubanyi, 1988].

Free radical scavengers increase SOD activity in MLDS-treated mice and alter the effects exerted by the diabetogenic drug on the islets, including the microvasculature [Papaccio et al., 1986]. On the other hand, an increased production of endothelial NO may be highly stimulated by hyperglycemia itself. NO is also involved in the anti-islet β cell attack and destruction (and a wide literature on the topic is available) but, when released by ECs, it is mainly involved in changes of vascular tone as it is a well-known vasodilator agent.

Our results demonstrate that iNOS mRNA transcripts are observed only in IL-1β treated ECs. Transcripts of eNOS, highly specific for endothelia, are significantly higher in 15-week-old animals (which are in the prediabetic state), with respect to both younger and older NOD mice. In fact, in younger (nondiabetic) and older (overtly diabetic) animals, values are comparable to those found in controls. A significant increase in eNOS mRNA levels is also observed in IL-10 treated ECs. This clearly confirms a direct action exerted by this cytokine upon islet ECs.

Nitrites and nitrates have been found to be a good index of the NO production state (i.e., as a marker for local NO production). In this study, a significant increase of NO production, due to increased levels of their stable metabolites, has been found in untreated NOD animals. This increase, due to a release of NO by islet ECs, is highly observed at week 15, when an increase of the peri-islet vascular bed (i.e., vessel dilation) occurs. Therefore, an activation of EC function, albeit locally, seems to happen, thus giving NO a paramount "vascular" role. The latter is also confirmed by the fact that IL-10 highly stimulates EC function by dilating peri-islet vessels: this activity is mirrored by the increase of plasma NO metabolites, which are an index of endothelial NO activation and by the increased levels of eNOS mRNA transcripts. On the other hand, IL-1β considerably accelerates diabetes development also increasing nitrite and nitrate levels in islet plasma, which become by the increase of iNOS mRNA transcripts.

Among cytokines, IL-4 and -10 have been demonstrated to exert an antidiabetogenic role, when administered both in vivo and in vitro [Rapoport et al., 1993]. IL-10, in particular, has been found to be also capable of activating ECs (i.e., enhancing eNOS transcripts) and induce leukocyte recruitment and extravasation in the pancreas [Wogensen et al., 1994]. These previous findings, therefore, strongly support our results, which demonstrate a sharper activity of this cytokine upon endothelia and vessels.

It has been found that IL-4 inhibits activated monocyte adhesion on ECs [Elliott et al., 1991] as well as the expression of adhesive molecules [Mantovani et al., 1992]. In this study, in vivo administration of IL-4 exerts a protective action against the microvascular, parenchymal, and biochemical alterations observed during the development of type 1 diabetes in NOD mice and downregulates circulating adhesive molecules. IL-10 is protective against type 1 diabetes development, although it exerts some activity upon endothelia and vessels, and, in addition, upregulates adhesion molecules, though limitedly to islet endothelia. IL-1β, a proinflammatory cytokine, accelerates type 1 diabetes development, including morphological and physiological changes. In fact, this cytokine worsens all values, with the exception of glycemia and antioxidant enzyme levels at the beginning of the treatment; actually, at this time, SOD values were unexpectedly stable, though they fell dramatically later on. This is an aspect which has been previously described in vitro [Borg et al., 1992], but, as here, it was only limited to the beginning of the cytokine challenge and seems to be due to a stimulation of islet β cells to secrete antioxidant enzymes. In addition, IL-1β strongly upregulates both soluble and cellular adhesion molecules.

The finding that both cytokines (IL-1β and -10) stimulate adhesion molecule expression is suggestive. In particular, while the IL-1β ICAM-1 upregulation could be explained by its inflammatory activity, that of IL-10 is rather complex to be interpreted. We think that its putative "vascular" role, as reported above, must be taken into consideration, as well as the finding that the upregulation is limited to islet ECs and scattered cells, and above all that it does not involve soluble adhesive molecules.

The different behavior of intra- and extra-islet vessel compartments during diabetes development and their contribution to islet cytoarchitectural derangement, demonstrated in this study, reveal that islet vessels are also involved in the natural history of type 1 diabetes and give a new insight for a possible vascular approach to early type 1 diabetes management. Targeting both vessels and, in particular, ECs during therapy could enable the combination

of different approaches in order to induce a shift from autoimmunity to self-tolerance. It is evident that upon exposure to cytokines, EC undergo profound alterations and actively participate in inflammatory reactions and immunity [Carlsson et al., 1997], although it must be stressed that vascular endothelia are quite heterogeneous both morphologically and functionally [Papaccio et al., 1998]. All these aspects, therefore, must be taken into consideration in future research on this topic.

ACKNOWLEDGMENTS

Campania Region (G.P.) funds (L.R. 31.12. 1994, n. 41) and PRIN 1999 funds (research projects of relevant interest, the Italian Ministry for Research and University) (G.P.) have supported this study.

REFERENCES

Bonner Weir S, Orci L. 1982. New perspectives on the microvasculature of the islets of Langerhans in the rat. Diabetes 31:883–889.

Borg LAH, Cagliero E, Sandler S, Welsh N, Eizirik D. 1992. Interleukin-1β increases the activity of superoxide dismutase in rat pancreatic islets. Endocrinology 130:2851–2857.

Carlsson P-O, Jansson L, Östenson C-G, Källskog Ö. 1997. Islet capillary blood pressure increase mediated by hyperglycemia in NIDDM GK rats. Diabetes 46:947–952.

Carlsson P-O, Sandler S, Jansson L. 1998. Pancreatic islet blood perfusion in the nonobese diabetic mouse: Diabetes-prone female mice exhibit a higher blood flow compared with male mice in the prediabetic phase. Endocrinology 139:3534–3541.

Chirgwin JM, Przybyla AE, MacDonald RJ, Rutter KT. 1979. Isolation of biologically active ribonucleic acid from sources enriched in ribonuclease. Biochemistry 18:5294–5299.

Cornelius JG, Luttge BG, Peck AB. 1993. Antioxidant enzyme activities in IDD-prone and IDD-resistant mice: A comparative study. Free Radic Biol Med 14:409–420.

Elliott MJ, Gamble JR, Park LS, Vadas MA, Lopez AF. 1991. Inhibition of human monocyte adhesion by interleukin-4. Blood 77:2739–2745.

Fiorentino DF, Bond MW, Mosmann TR. 1989. Two types of mouse helper T cell. IV. Th2 clones secrete a factor that inhibits cytokine production by Th1 clones. J Exp Med 170:2081–2095.

Gomori E. 1941. The distribution of phosphatase in normal organs and tissues. J Comp Physiol 17:71–84.

Gryglewski RJ, Botting RM, Vane JR. 1988. Mediators produced by endothelial cells. Hypertension Dallas 12:530–548.

Lowry OH, Rosebrough NJ, Farr AL, Randall RJ. 1951. Protein measurement with the Folin phenol reagent. J Biol Chem 193:265–275.

Mantovani A, Bussolino F, Dejana E. 1992. Cytokine regulation of endothelial cell function. FASEB J 6:2591–2599.

Marklund S, Marklund G. 1974. Involvement of the superoxide anion radical in the autooxidation of pyrogallol and a convenient assay for superoxide dismutase. Eur J Biochem 47:469–474.

Moore KV, O'Garra A, de Waal Malefyt R, Vieira P, Mosmann TR. 1993. Interleukin 10. Annu Rev Immunol 11:165–190.

Oellerich M, Engelhardt P, Schaadt M, Diehl V. 1980. Determination of methotrexate in serum by a rapid, fully mechanized enzyme immunoassay (EMIT). J Clin Chem Clin Biochem 18:169–174.

Papaccio G, Chieffi Baccari G. 1992. Alterations of islet microvasculature in mice treated with low dose streptozocin. Histochemistry 97:371–374.

Papaccio G, Pisanti FA, Frascatore S. 1986. Acetyl-homocysteine-thiolactone-induced increase of superoxide dismutase counteracts the effect of subdiabetogenic doses of streptozocin. Diabetes 35:470–474.

Papaccio G, Chieffi Baccari G, Mezzogiorno V, Esposito V. 1990. Capillary area in early low-dose streptozocin-treated mice. Histochemistry 95:19–21.

Papaccio G, Frascatore S, Pisanti FA. 1994. An increase in superoxide dismutase counteracts islet vascular alterations in low-dose streptozocin-treated mice. Histochemistry 101:215–221.

Papaccio G, Frascatore S, Pisanti FA, Latronico MGV, Linn T. 1995. Superoxide dismutase in the non obese diabetic mouse: A dynamic time-course study. Life Sci 56:2223–2228.

Papaccio G, Latronico MGV, Pisanti FA, Federlin K, Linn T. 1998. Adhesion molecules and microvascular changes in the nonobese diabetic (NOD) mouse pancreas. An NO-inhibitor (L-NAME) is unable to block adhesion inflammation-induced activation. Autoimmunity 27:65–77.

Pennline KJ, Roque-Gaffney E, Monahan M. 1994. Recombinant human IL-10 prevents the onset of diabetes in the nonobese diabetic mouse. Clin Immunol Immunopathol 71:169–175.

Rabinovitch A. 1988. An update on cytokines in the pathogenesis of insulin-dependent diabetes mellitus. Diabetes Metab Rev 14:129–151.

Rabinovitch A, Suarez-Pinzon WL, Sorensen O, Bleackley RC, Power RF, Rajotte RV. 1995. Combined therapy with interleukin-4 inhibits autoimmune diabetes recurrence in syngeneic islet-transplanted nonobese diabetic mice: Analysis of cytokine expression in the graft. Transplantation 60:368–374.

Rapoport MJ, Jaramillo A, Zipris D, Lazarus AH, Serreze DV, Leiter EH, Cyopick P, Danska JS, Delovitch TL. 1993. IL-4 reverses T-cell proliferative unresponsiveness and prevents the onset of diabetes in NOD mice. J Exp Med 178:87–99.

Rubanyi GM. 1988. Vascular effects of oxygen-derived free radicals. Free Radic Biol Med 4:107–120.

Steiner L, Krönke K-D, Fehsel K, Kolb-Bachofen V. 1997. Endothelial cells as cytotoxic effector cells: Cytokine-activated rat islet endothelial cells lyse syngeneic islet cells via nitric oxide. Diabetologia 40:150–155.

Svensson AM, Jansson L, Hellerström C. 1988. The volume and area of the capillaries in the endocrine and exocrine pancreas of the rat. Histochemistry 90:43–47.

Wogensen L, Huang X, Sarvetnik N. 1993. Leukocyte extravasation into the pancreatic tissue in transgenic mice expressing interleukin 10 in the islets of Langerhans. J Exp Med 178:175–185.

Wogensen L, Lee M-S, Sarvetnick N. 1994. Production of interleukin 10 by islet cells accelerates immune-mediated destruction of β cells in nonobese diabetic mice. J Exp Med 179:1379–1384.